



ELSEVIER

15 January 2002

Optics Communications 201 (2002) 363–372

OPTICS
COMMUNICATIONS

www.elsevier.com/locate/optcom

m-lines technique application for studying of optical nonlinearities in thin films at a low light intensity

Alexander V. Khomchenko*

Institute of Applied Optics NASB, 11 Belynskogo-Biruly St., 212793 Mogilev, Belarus

Received 25 July 2001; accepted 2 November 2001

Abstract

In the range of a light intensity below 0.1 W/cm^2 nonlinear optical properties of semiconductor and dielectric thin films are studied at a wavelength of 632.8 nm. Optical nonlinearity was investigated by the technique of the spatial Fourier spectroscopy of guided modes excited in these thin-film structures in the self-effect case. The nonlinear refractive index and the absorption coefficient were found to be about $10^{-3} \text{ cm}^2/\text{W}$ for semiconductor films and multilayer structures and about $10^{-6} \text{ cm}^2/\text{W}$ for quartz glass films. Origin of this optical nonlinearity is considered as a photo-induced modification of surface states in the optical band gap. © 2002 Published by Elsevier Science B.V.

Keywords: *m*-lines; Fourier spectrum; Optical nonlinearity; Thin film; Interface

1. Introduction

Studying of the nonlinear propagation of light beams in thin films is of greater interest because of a wide range of possible applications of this phenomenon in optoelectronic devices, photonic switching as well as because of new fundamental physical mechanisms which are typical for these structures [1–3]. Also thin-film structures can serve as models to study fundamental aspects of electromagnetic fields and nonlinear materials cointeraction [4].

Often success in thin film physics is caused by the development of new investigation methods. The prism coupler technique, also referred to as the *m*-lines technique, is commonly used to determine the optical parameters of thin films [5,6]. Improvement of existing waveguide techniques of thin film parameter measurements and development of new ones make it possible to study the nonlinear optical properties of guiding films [7–9].

In this paper the studying results of the optical nonlinearity in thin films and low dimensional structures in the photon energy range below optical band edge are presented. Nonlinear changes in refractive index and in absorption coefficient of waveguiding films at the incident light beam intensity below 0.1 W/cm^2 were recorded.

* Fax: +375-222-264649.

E-mail address: avkh@physics.belpak.mogilev.by (A.V. Khomchenko).



2. Thin film fabrication

The polycrystalline and amorphous semiconductor films, multilayer structures, dielectric and semiconductor-doped glass thin films, which had been fabricated by the vacuum deposition methods, were used as the samples under investigation.

The chalcogenide glass (As_2S_3) films were made by thermal evaporation. By RF sputtering made the ZnSe films, SnO_2 films, the semiconductor-doped glass (SDG) films and the quartz glass films. Multilayer structures were obtained by alternative sputtering of conductor and dielectric materials. Lithium niobate and tin dioxide were used as conductor, quartz glass was used as dielectric. In multilayer structures the layers of quartz glass, lithium niobate, and tin dioxide had thicknesses of 20–70, 30–50, and 10–80 nm, and refractive indices of 1.476, 2.16, and 1.99, respectively. The layer thickness in these structures was controlled by the deposition time. The tin dioxide layers and ZnSe films were prepared by sputtering of ceramic target, sputtering of monocrystalline target made the lithium niobate layers. Oxygen content in the sputtering atmosphere was varied from 10 to 20 vol% in the Ar– O_2 mixture. All films were deposited on quartz glass substrates at pressure of 10^{-3} Torr. The SDG films were obtained by sputtering of an OS12 glass target ($\text{CdS}_x\text{Se}_{1-x}$ -doped glass) in an argon atmosphere. The substrate temperature did not exceed 250 °C.

3. Measuring the linear and nonlinear optical parameters of thin films

The optical parameters of thin films (the refractive index and the absorption coefficient) were determined by the prism-coupling technique. This approach is based on recording of the spatial intensity distribution (the angular Fourier spectrum) of the light beam reflected from the prism in case of excitation of a guided mode in thin-film structures by prism coupler and on determining of the complex mode propagation constant h ($h = h' + ih''$, $h' = \text{Re}h$, $h'' = \text{Im}h$) from the result processing of this distribution. In experiments, the resonant coupling of the laser beam into the waveguiding

film is observed through the appearance of a dark m -line in the reflected beam [5]. Each dark line has the its own spatial intensity distribution (in direction, which is normal to observable m -line) [8]. This distribution can be recorded at the appropriate installation of setup parameters.

The experimental setup is shown in Fig. 1. A linearly polarized He–Ne laser at wavelength of 632.8 nm is used as the light source in the prism coupler. Being partially reflected from the prism base, the incident laser beam is coupled by the prism into a planar waveguide. Under total internal reflection conditions on the prism base, strong coupling of light into the waveguide can occur via resonant frustrated total reflection, i.e. via evanescent waves in an air gap between the prism and the waveguide. Being propagated along the film, the light beam is radiated into the prism and one is interfered with the reflected beam.

Thus the output light beam comprises the information about the sample under investigating. When determining film parameters the results of processing of the spatial intensity distribution of this light beam were used.

The spatial distribution of the reflected light beam intensity was measured by the matrix

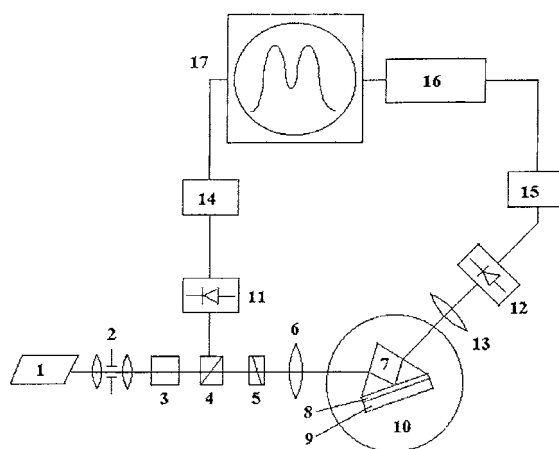


Fig. 1. Experimental setup used for determination of optical parameters of thin-film waveguides: 1 – light source, 2 – collimator, 3 – attenuator, 4 – beam splitter, 5 – polarizer, 6, 13 – lens, 7 – prism coupler, 8 – gap, 9 – waveguide, 10 – rotate table, 11, 12 – photodetectors, 14, 15 – intensity measuring device, 16 – analog digital converter, 17 – PC.

photodetector (12) connected to a digital image processing system (16). Its rotation axis is connected to the rotation axis of the spectroscopic goniometer table (10). The light beam propagates through lens (13), whose focus plane coincides with location of photodetector. These design features provided the recording of the angular Fourier spectrum of the reflected light beam. The recorded parameter is the reflected light beam power b for fixed angle φ_j . The measurement error of the angle and light intensity due to the experimental setup made 2×10^{-5} and 0.1%, respectively.

Typical intensity distribution of the reflected light beam in case of excitation of the guided mode by the prism couple (7) is presented in Fig. 2(a) (curve 1). This distribution is recorded along direction, which is normal to observable m -line. Here the angle φ is the angle between the incidence of a plane wave and the mean incidence of the Gaussian beam. The measured intensity dependence on the angle is a resonant curve $b(\varphi)$ with certain half width.

Determination of the extreme coordinates of the $b(\varphi)$ dependence recorded experimentally in discrete points φ_j ($j = 1, 2, \dots, l$) assumes interpolation of this function. Interpolation was made by the normal regression analysis [10]. In this case an accuracy of determination of an optimum angle φ_{\min} of the mode excitation was 2×10^{-6} .

For m -lines techniques the coupling between the prism and the waveguide is generally considered weak and is neglected as soon as the thickness of the air gap between the prism and the waveguide is greater than about half the incident light wavelength [11,12]. But in this case the prism's influence on the measuring results was taken into account. Moreover, used approach allows determination of the thickness of the air gap as well as part of the light power coupled into the thin film. After processing of the obtained distribution one can reconstructed real and imaginary parts of propagation constants of the free guided modes [8]. The real part of h is determined from a resonant minimum in the angular dependence of the light reflection coefficient φ_{\min} , an angular width of a resonant minimum $\Delta\varphi$, and a contrast of recorded distribution $V = (b_{\max} - b_{\min})/b_{\max}$. Here $b_{\min} = b(\varphi_{\min})$, $b_{\max} = b(\varphi_{\max})$ and $\Delta\varphi = (\varphi_{\max} - \varphi_{\min})$.

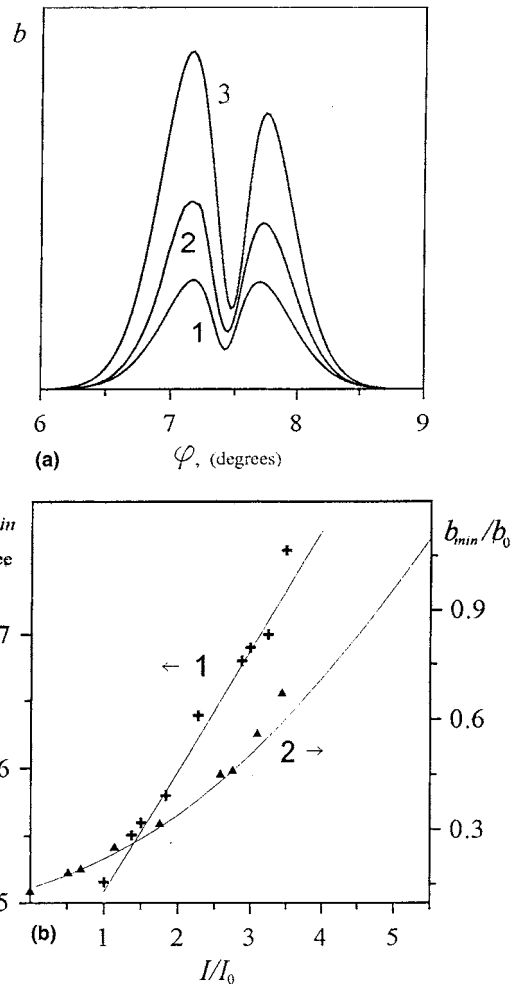


Fig. 2. Changes in the angular Fourier spectrum of the light beam, reflected from the prism base in case of excitation of a guided mode in the thin-film structure, caused by increasing of the light intensity ((a): $I = I_0$ (1), $I = I_1$ (2), $I = I_2$ (3), $I_2 > I_1 > I_0$), and dependencies of φ_{\min} and b_{\min}/b_0 on relative intensity I/I_0 (b).

The imaginary part of propagation constant is determined from V and $\Delta\varphi$.

The refractive index n , the absorption coefficient k and the film thickness d can be calculated from the measured h for any two modes [13].

Absorption spectra of thin films were also measured by the waveguide spectroscopy technique using a noncoherent light source in setup given in Fig. 1. The using of the wide light beam

(in angles) at measuring and of the gradient method of optimization (steepest descent) at determining of h has allowed to avoid additional positioning of the prism in case of a changing of a incident light frequency. It is possible to determine the absorption coefficient of the film material in a visible range of the spectrum. Details of the waveguide spectrometer and measurements can be found elsewhere [14].

The nonlinear refractive index n_2 and the nonlinear absorption coefficient k_2 were measured by waveguide method at a wavelength of 632.8 nm, too. This approach is based on the transformation of the Fourier spectrum of the reflected light beam in the self-effect case [9]. The measurement technique is identical to the one of the linear parameter measurement. Measurements were made on the same setup (Fig. 1). It should be noted that the using of an intensity measurement device (11) and an attenuator (3), which were added into setup, has allowed changing and testing the light intensity I . The incident light power was changed in the range from 0.5 to 500 μW . The radius of the light beam at the prism base did not exceed 300 μm . The estimations of the optical parameter variations caused by increase in the film's temperature due to light absorption were executed according to [16] and in all cases these changes were by an order of magnitude less the h' measurement errors.

The changes in intensity distribution of the reflected beam are a result of the gradual increase in the light intensity (Fig. 2(a), curves 1–3). Curve 1 describes the case, when the power of the incident light was reduced as much as possible by ND filters and was equal to 0.5 μW . At this power level ($I = I_0$), photo-induced changes in films by red light were hardly observed. The angular coordinate φ_{\min} of the intensity minimum in the intensity distribution and the intensity minimum b_{\min} of the recorded distribution $b(\varphi)$ are changed during of gradual increase in the light intensity.

Dependencies φ_{\min} and b_{\min}/b_0 as functions of (I/I_0), which were obtained by processing of the recorded angular Fourier spectra (see Fig. 2(a)), are shown in Fig. 2(b), where $b_0 = b_{\min}$ under conditions $I = I_0$ (Fig. 2(a), curve 1). A complex nonlinear parameter of the waveguide was determined from results of processing these dependen-

cies. Using the complex nonlinear parameter, the previously calculated n , d and the field distribution of the guided mode the nonlinear n_2 and k_2 were determined [9].

4. Nonlinearity of optical properties of semiconductor films

When studying optical nonlinearity in thin films from chalcogenide glass (As_2S_3) the nonlinear optical constants n_2 and k_2 were measured in an incident light intensity range from 10 to 100 W/cm^2 [9]. In this case $n_2 = 1.5 \times 10^{-5} \text{ cm}^2/\text{W}$ and results of other researches [15] were satisfactorily correlated.

But in a range of the incident light intensity below 0.1 W/cm^2 the strong nonlinear dependence of optical parameters on the intensity was indicated. The $\Delta h'$ dependence on the incident light intensity I for the guided mode excited in the As_2S_3 film is shown in Fig. 3 (curve 1), where $\Delta h'(I) = h'_n(I) - h'(I_0)$. Here and below h'_n relate to the measurable synchronous angle θ of guided mode as $h'_n = k_0 n_p \cos \theta$, where n_p is the refractive index of the prism coupler, k_0 is the free space wave number. In the linear case h'_n is the real part of the mode propagation constant. The measured

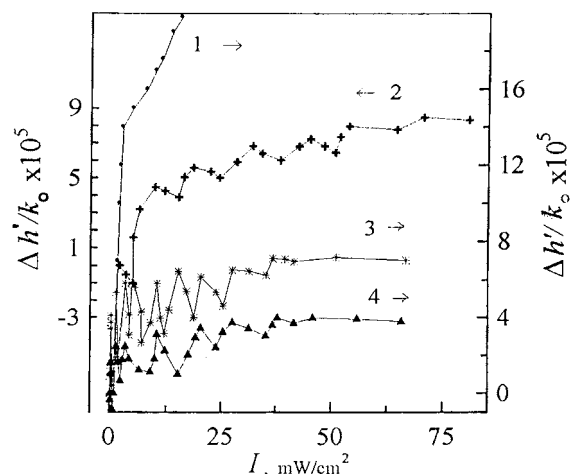


Fig. 3. Dependencies $h'(I)$ for films from As_2S_3 (1) and for the ZnSe films deposited under substrate temperature 180 $^\circ\text{C}$ (2), 240 $^\circ\text{C}$ (3) and 280 $^\circ\text{C}$ (4).

magnitude of n_2 was equal to $2.65 \times 10^{-3} \text{ cm}^2/\text{W}$. In this case variations of optical parameters caused by increase in the film's temperature due to light absorption were much smaller (of about 10^{-8}) than the observed changes in refractive index. It confirms a non-thermal origin of the optical nonlinearity being observed [16].

Nonlinear changes resulted from low light intensity variations were observed in ZnSe films. The $\Delta h'$ intensity dependencies for these films deposited at the various substrate temperature 140, 180, 250 °C (curves 2, 3 and 4, respectively) are shown in Fig. 3. In this case a common tendency of a decrease in h' and absorbance (decrease in h'') is observed. The measuring error of $\Delta h'$ was 2×10^{-6} . These curves are non-monotonic and have complex behavior. Analyses of obtained results show that behavior of dependencies $h'_n(I)$ and values of the nonlinear constant n_2 were defined by the crystal quality of thin films. The ZnSe films were polycrystalline and in all cases their crystallites had the cubic structure, which is primary orientated in the direction (0 2 2) being parallel to the substrate surface. When identified the X-ray diffraction spectra other structures are not revealed. In these films, the mean sizes of a single crystallite were 19, 7 and 12 nm [17] (Fig. 3, curve 2, 3 and 4, respectively).

5. Optical nonlinearity in semiconductor-doped glass thin films

Similar nonlinear changes resulted from low light intensity variations were observed in thin films obtained by sputtering of SDG. A complex shape of dependence $h'(I)$ is distinctly seen (Fig. 4) and a magnitude of its variations greatly exceeds the measurement error. It should be noted that in this case a common tendency of a decrease in h' and an increase in absorbance is observed [18].

Optical nonlinearity in materials of this kind is defined by semiconductor crystallites embedded in a glass matrix [3]. Optical properties of SDG depend on the crystallite size, which can be varied by thermal annealing or deposition conditions. Thin-film waveguides from this glass were heated at temperature 500 °C in vacuum for 4 h. The results

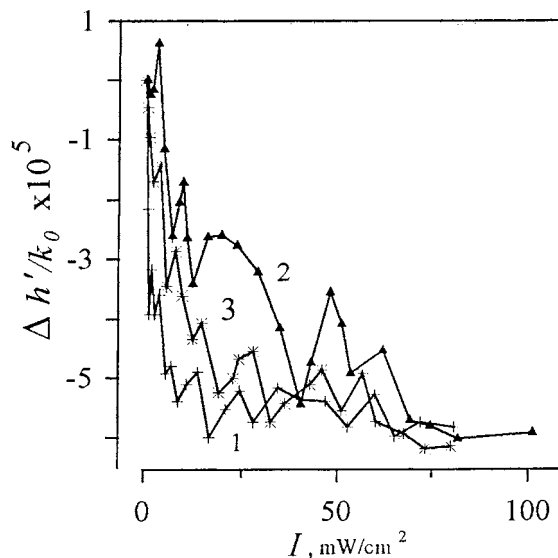


Fig. 4. Changes in parameters of the thin-film waveguides obtained by sputtering of the semiconductor-doped glasses versus the incident light intensity I : before (1) and after (2) thermal annealing and deposited at the substrate temperatures of 140 °C (1) and 190 °C (3).

of measurements of waveguide parameters before and after annealing are presented in Fig. 4 (curves 1 and 2). The increased substrate temperature at the film deposition results in the same changes (Fig. 4, curve 3).

The SDG-films obtained at small deposition rate had stoichiometry composition and effect of film bleaching during a gradual increase in the incident light beam intensity is observed.

Optical nonlinearity at the low light intensity was also observed in dielectric films, not containing $\text{CdS}_x\text{Se}_{1-x}$ crystallites. In thin films obtained by RF sputtering of quartz glass the nonlinear changes of their optical properties caused by increasing of the light intensity were recorded. In this case n_2 was much below, than in semiconductor films or in SDG-films, and made $\sim 10^{-4} \dots 10^{-7} \text{ cm}^2/\text{W}$. However nonlinear dependence of optical parameters on incident light intensity was reliably recorded only in films with distorted stoichiometry.

When the optical losses in guiding film were equal to $\sim 2 \text{ dB/cm}$ this effect was not indicated (see Fig. 5).

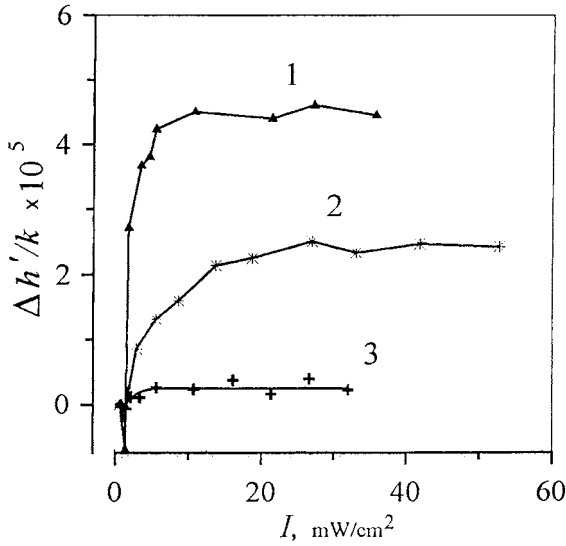


Fig. 5. Intensity dependence of h' for the quartz glass films with $k = 2 \times 10^{-5}$ (1), 9×10^{-6} (2) and 3×10^{-6} (3).

6. Optical properties of multilayer structures

The intensity dependencies of optical properties were investigated in noncrystalline and polycrystalline semiconductor films, SDG and dielectric films. The optical band edge (in wavelengths) for these materials not always was equal to the wavelength of incident light, and nonlinear changes of optical properties were recorded in all structures. That is why the optical nonlinearity in thin-film structures can be caused by interface effect [3,17].

From this point of view it is interesting to try modeling some nonlinear system, which has a large number of interfaces and can be made as a multilayer structure [19]. Two kinds of multilayer structures were used. The first structure was made by alternative deposition of lithium niobate (a conductor) and quartz glass (a dielectric). The conducting layers are isolated from each other by dielectric layers. The intensity dependence of h'_n for these structures is shown in Fig. 6. The represented curves are non-monotonic and have complex shapes.

Moreover, h'_n functions have five extremes for structures having five lithium niobate layers. When exciting guided modes in the structure having three

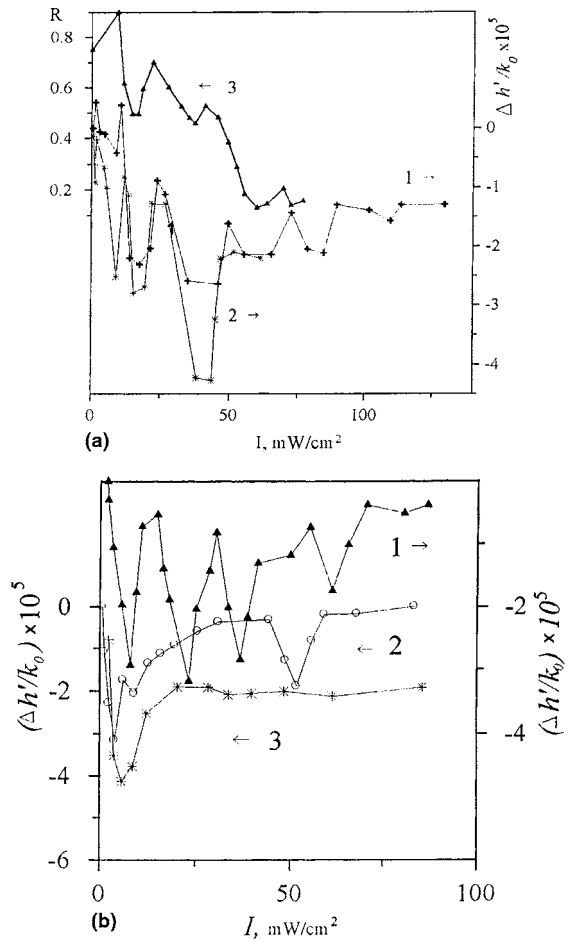


Fig. 6. Variations of the real part of the mode propagation constant h' as function of the incident light intensity I for (a): the multilayer structure containing three (1), five (2) and six (3) lithium niobate layers and (b): the multilayer structure containing three (1) and one tin dioxide layer in air (2) and water vapors (3).

lithium niobate layers the h'_n functions have three peaks. And in case of exciting guided modes of various polarizations, the similar function behavior was observed, too. The intensity dependence of a light beam reflection coefficient was also non-monotonic, as it is shown in Fig. 6(a) (curve 3). The diameter of the incident light beam was $290 \mu\text{m}$.

Using processing results of changes in the recorded intensity distribution during gradually increasing the light intensity, one can determine the nonlinear constants n_2 and k_2 in different intensity

ranges: $n_2^{(1)} = -2.1 \times 10^{-3} \text{ cm}^2/\text{W}$, $k_2^{(1)} = 5.1 \times 10^{-3} \text{ cm}^2/\text{W}$, $n_2^{(II)} = 3.1 \times 10^{-3} \text{ cm}^2/\text{W}$, $k_2^{(II)} = -6.2 \times 10^{-3} \text{ cm}^2/\text{W}$ (Fig. 6, curve 1).

Other multilayer structures were made by alternative deposition of linear optical materials such as tin oxide and quartz glass. This structure having a separate layer thickness of about 10 nm simulated a low dimensional structure. The dependence $\Delta h'(I)$ for this multilayer structure containing three layers of tin dioxide isolated from each other by quartz glass layers is shown in Fig. 6(b) (curve 1). This curve has three recorded extremes, too.

From presented results it follows that the number of layers in the studying sample defines the complex shape of the $h'_n(I)$ function.

The thickness d_l of tin dioxide layers in the second structure was 12, 24 and 36 nm. The thickness of sputtered layers was controlled by deposition time. It is evident that the wider minimum of $h'_n(I)$ corresponds to the greater layer thickness. The shape of the third peak ($d_l = 36 \text{ nm}$) is similar to that of the $h'_n(I)$ function for the thicker film ($d_l = 120 \text{ nm}$) shown in Fig. 6(b) (curve 2), i.e., when the layer thickness exceeds $\sim 30 \text{ nm}$, the nonlinear response from each interface of this layer can separately be recorded.

The nonlinear optical properties of multilayer structures depended on optical quality of dielectric layers. The intensity dependencies of h'_n for three tin dioxide films deposited on different substrates at identical conditions during the same deposition process are shown in Fig. 7. Here, quartz glass and structures “SiO_x film – quartz glass” were used as substrates. The SiO_x films being deposited at various conditions had a different composition, that is why they had different absorption coefficient k of 1.5×10^{-5} (curve 2) and 5.0×10^{-6} (curve 3), respectively. The SiO_x film thickness was 1 μm . It is known that even a neutral amorphous substrate affects the thin-film waveguide property [20]. And in this case the nonlinearity changes in optical properties were greater in waveguide structures containing the dielectric film with greater k as a buffer layer between the substrate and the waveguide.

These results show that the interfaces define a non-monotonic intensity dependence of the thin-film optical properties.

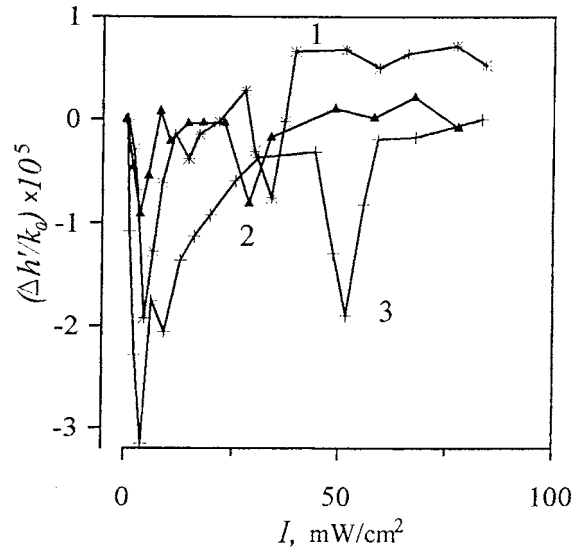


Fig. 7. Intensity dependence of h' for the multilayer structures: “SnO₂-film – quartz glass” (1), “SnO₂ film – SiO_x film – quartz glass”, where the absorption coefficients of SiO_x films are 1.5×10^{-5} (curve 2) and 5×10^{-6} (curve 3).

The additional information on processes causing the optical nonlinearity in thin films one can obtain from spectral measurements. Absorption spectra of the SnO₂ film up to and during the additional illumination of film by the laser light beam (wavelength of $0.6328 \mu\text{m}$) are presented in Fig. 8 (curves 1 and 2, respectively). The curve 3 shows absorption spectrum of this film in the water vapor. All spectral dependencies are obtained by the waveguide spectroscopy method [14]. From an analysis of these results the presence of free power levels in optical band gap follows.

If origin of optical nonlinearity is associated with a modification of surface states, the behavior of $h(I)$ can be changed by pumping of a gas in the thin film surrounding. The realization of this experiment is stipulated by the fact that at each internal reflection in the waveguide the interference between incident and reflected internal beam creates a nonpropagating standing wave, which is normal to the reflecting surface. The energy associated with this wave tails out into surroundings where it can interact with gas molecules. Chemisorption of a gas on a semiconductor, in particular, results in a change of power states in the band



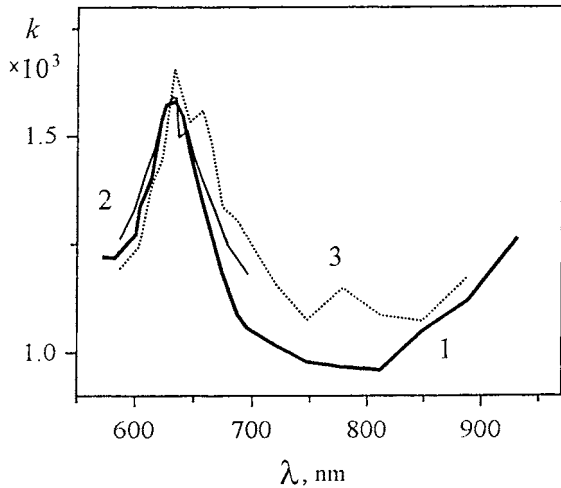


Fig. 8. Absorption spectra of the SnO_2 film: before (1) and during (2) additional illumination by the laser light ($\lambda = 0.63 \mu\text{m}$), in water vapors (3).

gap [21,22]. To make this experiment, the waveguide structure consisting of silicon dioxide and tin dioxide films, which were successively deposited on the base of the prism coupler, was fabricated. Since water vapor actively saturate levels of surface states [23], one can expected the observed decrease in absorbance (and the increase in h') to be suppressed in the film in the water vapor atmosphere.

The results of these measurements in water vapor atmosphere and in air are presented in Fig. 6(b) (curves 3 and 2, respectively). It can be seen that decrease in the refractive index (and increase in absorbance) in the range of low intensities of the incident light was present in each cases, but a bleaching of the film in water vapor atmosphere was not observed. Here it should be noted that decrease in h'_n during gradually increasing the incident light intensity corresponds to the decrease in the refractive index. Thus, the assumption of the interface influence on the nonlinearity of optical properties is proved to be quite correct.

7. Discussions

The analysis of represented results and results of another researchers [15,24] show that the photo-

induced changes in optical properties of the thin films are a result of some photoelectronic effects. Its origin is considered as a modification of surface states in the band gap.

Apparently, the guided mode propagates in all layers of the thin-film structure and the mode field distributions for various light intensities are identical (at least, at small I). But when $I = I_0$ the mode amplitude is so small that nonlinear effects are not yet displayed or, already to be more correct, are not recorded by the available setup. By gradually increasing the intensity, one can indicate the nonlinear response from the one interface, then from two, etc. Thus, if $|k_2^{(I)}| > |k_2^{(II)}|$ in the structure, the electron processes involved on each of subsequent interface increase the total absorption in the multilayer structure. Accumulating this effect, the structure tends to increase the absorption coefficient during augmentation of the incident light beam intensity. Otherwise, at $|k_2^{(I)}| < |k_2^{(II)}|$ the effect of film bleaching is observed [19].

The above considerations can be applied to the SDG films, too. But in this case the surface of the semiconductor crystallite embedded in glass matrix should be consider as the “semiconductor-dielectric” interface. Some models have been offered to explain the entire set of phenomena occurring under irradiation of $\text{CdS}_x\text{Se}_{1-x}$ -doped glasses. One of them considers the escape of an electron from the crystallite into the matrix and the subsequent trapping of the electron on localized states in the band gap of the glass. The filling of localized levels in the glass matrix induces absorption in the impurity-band channels, which results in the appearance of additional absorption in the visible range of the spectrum [15].

In [24,25] the refractive index and absorption coefficient decrease in SDG waveguides is revealed. Negative n_2 is explained on the basis of the mechanism of band filling. In this case [25], the non-monotonic behavior of the $n(I)$ dependence is also observed and this fact is connected to saturation of the electronic mechanism of optical nonlinearity. Here it should be noted that the thermal effect results to an increase in refractive index.

Thus the photo-induced changes in optical properties of thin films, multilayer structures and

semiconductor-doped glass films have a common origin and it is probable that these changes are caused by the generation of a sufficient number of electron–hole pairs during the film illumination by laser light. In this case equation of a carrier balance near to the film surface is

$$g_s = \frac{1}{e} j_s(0) + s_r,$$

where g_s is a rate of the surface carrier generation, s_r is a rate of the carrier decrease caused by a surface recombination, $j_s(0)$ is a carrier current near the film surface [26].

The equation is written down in approach $g_s = C$ at any absorption coefficient of the film material, where C is some constant. As the photon energy is below than optical band gap and the concentration of surface states can achieve equal to number of atoms at the film surface, $j_s(0) < 0$. In this case the carrier current is directed to the semiconductor surface.

The behavior of the intensity dependence of optical properties of thin-film structures allows the following assumption to be made. With a large degree of reliability the region of the absorption increase (Fig. 6(a), Section 1) can be related to the trapping of the light generated non-equilibrium carriers in localized states in the optical band gap. The filling of localized levels produces an absorption in the visible range of the spectrum. At the same time a cross-section for the carrier capture by defects is changed as a result of the charged defect localized near the surface. Also it is should be noted, that some surface states are not localized. A part of them participates in recombination processes. The filling of free power levels of surface states stimulates the absorption decrease in films. Then the process photodarkening in thin-film structures can be interpreted within a two-level power model optical recharging of the localized states in the band gap [15,27], and the bleaching of films can be explained on the basis of effect of “band filling” [2,25].

Thus, the nonlinear changes in the optical properties of these structures can be a result of a photostimulated migration of non-equilibrium carriers out of the film volume to the interface, of subsequent carrier trapping in localized states as

well as of carrier recombination. These processes define the non-monotonic behavior of the intensity dependence of optical properties in the thin-film structures.

8. Conclusions

In a range of light intensities below 0.1 W/cm^2 the nonlinear optical properties of semiconductor thin films, multilayer structures, semiconductor-doped glass films and dielectric films are studied by the technique of the spatial Fourier spectroscopy of guided modes excited in these structures. The nonlinear refractive index and the nonlinear absorption coefficient were found to be about $10^{-3} \text{ cm}^2/\text{W}$ at a wavelength of 632.8 nm. Use of such approach allowed the nonlinear response from each interface of the layer in multilayer structure separately to record. Common tendencies in intensity dependencies of optical properties of thin-film structures were studied. It was shown that the state of interfaces determines the optical nonlinearity behavior at the low light intensity.

Acknowledgements

This research was supported by the Belarus Republic Foundation of Basis Research.

References

- [1] G.I. Stegeman, C.Y. Seaton, *J. Appl. Phys.* 58 (1985) R57–R78.
- [2] H. Gibbs, *Optical Bistability: Controlling Light with Light*, Academic Press, Orlando, Moscow, Mir, 1988, Chapter 5.
- [3] S.V. Gaponenko, *Optical Properties of Semiconductor Nanocrystal*, University Press, Cambridge, 1998, Chapter 7.
- [4] D.A.B. Miller, D.S. Chemla, T.C. Damen, A.C. Gossard, W. Wiegmann, T.H. Wood, C.A. Burrus, *Phys. Rev. B* 32 (2) (1985) 1043–1060.
- [5] P.K. Tien, R. Ulrich, R.J. Martin, *Appl. Phys. Lett.* 14 (9) (1969) 291–294.
- [6] S. Monneret, P. Huguët-Chantome, F. Flory, *J. Opt. A: Pure Appl. Opt.* 2 (2000) 188–195.
- [7] H. Rigneault, F. Flory, S. Monneret, *Appl. Opt.* 34 (1995) 4358–4369.
- [8] V.P. Red’ko, A.A. Romanenko, A.B. Sotsky, A.V. Khomchenko, *Sov. Techn. Phys. Lett.* 18 (4) (1992) 14.



- [9] A.B. Sotsky, A.V. Khomchenko, L.I. Sotskaya, *Techn. Phys. Lett.* 20 (8) (1994) 667–669.
- [10] B.R. Friden (Ed.), *The Computer in Optical Research. Methods and Applications*, Springer, Berlin, 1980 (1983, Chapter 4).
- [11] R. Ulrich, R. Torge, *Appl. Opt.* 12 (1973) 2901–2908.
- [12] R.T. Kersten, *Opt. Acta* 22 (1975) 503–521.
- [13] A.B. Sotsky, A.A. Romanenko, A.V. Khomchenko, I.U. Primak, *J. of Comm. Techn. and Electr.* 44 (6) (1999) 640.
- [14] A.V. Khomchenko, *Techn. Phys. Lett.* 27 (4) (2001) 271–274.
- [15] A. Andriesh, V. Chumash, *Pure Appl. Opt.* 7 (1998) 351–360.
- [16] A.B. Sotsky, A.V. Khomchenko, L.I. Sotskaya, *Opt. Spectrosc.* 78 (4) (1995) 502–511.
- [17] A.V. Khomchenko, *Techn. Phys.* 42 (1997) 1038.
- [18] A.V. Khomchenko, *Techn. Phys.* 45 (2000) 1505–1508.
- [19] A.V. Khomchenko, E.V. Glasunov, *Opt. Quantum Electron.*, to be published.
- [20] A.V. Khomchenko, V.P. Red'ko, in: A.M. Prokhorov, E.M. Zolotov (Eds.), *Proc. SPIE*, 1932, 1993, pp. 14–23.
- [21] V.F. Kisel'ov, O.V. Krilov, *Electronic Phenomena in Adsorption and Catalysis*, Springer, New York, 1986, Chapter 5.
- [22] V.M. Aroutiounian, G.S. Aghababian, *Appl. Surf. Sci.* 135 (1998) 1–7.
- [23] A. Madan, M.P. Shaw, *The Physics and Applications of Amorphous Semiconductors*, Academic Press, Boston, 1988, Chapter 2.
- [24] K.S. Bindra, S.M. Oak, K.C. Rustagi, *Pure Appl. Opt.* 7 (1998) 345–349.
- [25] W.S. Banyai, C.T. Seaton, G.I. Stegeman, M. O'Neill, T.J. Cullen, et al., *Appl. Phys. Lett.* 54 (6) (1989) 481–483.
- [26] V.L. Bonch-Bruевич, C.G. Kalashnikov, *The Physics of Semiconductors*, Nauka, Moscow, 1977, Chapter 10.
- [27] J. Malhotra, D.J. Hagan, B.G. Potter, *J. Opt. Soc. Am. B* 8 (1991) 1531–1536.

